



This is a repository copy of *A GaAsSb/AlGaAsSb avalanche photodiode with a very small temperature coefficient of breakdown voltage.*

White Rose Research Online URL for this paper:

<https://eprints.whiterose.ac.uk/185805/>

Version: Accepted Version

Article:

Cao, Y. orcid.org/0000-0002-6353-7660, Osman, T., Clarke, E. orcid.org/0000-0002-8287-0282 et al. (3 more authors) (2022) A GaAsSb/AlGaAsSb avalanche photodiode with a very small temperature coefficient of breakdown voltage. *Journal of Lightwave Technology*, 40 (14). pp. 4709-4713. ISSN 0733-8724

<https://doi.org/10.1109/jlt.2022.3167268>

© 2022 IEEE. Personal use of this material is permitted. Permission from IEEE must be obtained for all other users, including reprinting/ republishing this material for advertising or promotional purposes, creating new collective works for resale or redistribution to servers or lists, or reuse of any copyrighted components of this work in other works. Reproduced in accordance with the publisher's self-archiving policy.

Reuse

Items deposited in White Rose Research Online are protected by copyright, with all rights reserved unless indicated otherwise. They may be downloaded and/or printed for private study, or other acts as permitted by national copyright laws. The publisher or other rights holders may allow further reproduction and re-use of the full text version. This is indicated by the licence information on the White Rose Research Online record for the item.

Takedown

If you consider content in White Rose Research Online to be in breach of UK law, please notify us by emailing eprints@whiterose.ac.uk including the URL of the record and the reason for the withdrawal request.



eprints@whiterose.ac.uk
<https://eprints.whiterose.ac.uk/>

A GaAsSb/AlGaAsSb Avalanche Photodiode with a very small Temperature Coefficient of Breakdown Voltage

Ye Cao, Tarick Osman, Edmund Clarke, Pallavi Kisan Patil, Jo Shien Ng, *Member, IEEE*,
and Chee Hing Tan, *Senior Member, IEEE*

Abstract—Avalanche photodiodes (APDs) made with the material AlGaAsSb (lattice-matched to InP) exhibit very low excess noise characteristics. We demonstrate a Separate Absorption and Multiplication APD (SAM-APD) incorporating a GaAs_{0.52}Sb_{0.48} (GaAsSb) absorption region and an Al_{0.85}Ga_{0.15}As_{0.56}Sb_{0.44} (AlGaAsSb) avalanche region. Our GaAsSb/AlGaAsSb SAM-APD exhibits a cut-off wavelength of 1.70 μm at room temperature and a responsivity of 0.39 A/W at 1.55 μm wavelength (with no antireflection coating). Temperature dependence of the breakdown voltage was obtained from avalanche gain data from multiple devices operated at 77 to 295 K. This produced a temperature coefficient of breakdown voltage of 4.31 ± 0.33 mV/K, a factor of 10 and 5 smaller than values for comparable InP and InAlAs SAM-APDs. The very small temperature coefficient of this work is consistent with the extremely weak temperature dependence of avalanche breakdown previously observed in AlGaAsSb diodes.

Index Terms—Avalanche photodiode (APD), avalanche breakdown, AlGaAsSb, GaAsSb, impact ionization, Separate Absorption and Multiplication Avalanche Photodiode (SAM-APD), temperature coefficient.

I. INTRODUCTION

AVALANCHE photodiodes (APDs) have been used to detect incoming optical signals in a wide range of applications, such as optical communication, imaging, and single-photon detection for quantum key distribution. The main advantage of APDs over conventional photodiodes is the APD's internal gain, which enhances the signal-to-noise ratio of an APD-preamplifier module. The internal gain, termed avalanche gain, M , is the result of successive impact ionization events that take place within the APD's avalanche region (typically under high electric fields).

Since impact ionization events are stochastic, the avalanche gain brings additional noise relative to shot noise. This is

usually quantified by the excess noise factor, F , which tends to increase with M . $F(M)$ characteristic is, therefore, an important APD performance parameter. It is strongly dependent on the ratio of impact ionization coefficients, $k = \beta/\alpha$ [1], where α and β are the impact ionization coefficients of electrons and holes, respectively.

Semiconductor materials with $k \sim 0$ exhibit very low excess noise and examples include Si [2], InAs [3] and Hg_{0.7}Cd_{0.3}Te [4]. Hence Si APDs are the dominant APDs for applications operating in the 400-1000 nm wavelength range. InAs and Hg_{0.7}Cd_{0.3}Te have narrow band gaps, leading to relatively high dark currents at room temperature and operation at lower than room temperature. This limits their use in room temperature applications in the 1.3-1.6 μm wavelength range. For this infrared wavelength range, the APDs of choice are the Separate Absorption and Multiplication Avalanche Photodiode (SAM-APD). It combines an In_{0.53}Ga_{0.47}As (hereafter referred to as InGaAs) absorption region with either an InP [5], or more recently an In_{0.52}Al_{0.48}As [5] avalanche region. However, both InP [7] and In_{0.52}Al_{0.48}As [8] have k approaching unity under high electric fields, so their $F(M)$ characteristics are much higher compared to Si.

In recent years, excellent experimental $F(M)$ characteristics from APDs made using Sb-containing materials have been reported. AlAs_{0.56}Sb_{0.44} (lattice-matched to InP substrate) exhibited extremely low excess noise with effective $k \sim 0.005$ [9] to 0.05 [10]. $F(M)$ characteristics of Al_{0.85}Ga_{0.15}As_{0.56}Sb_{0.44}, (hereafter referred to as AlGaAsSb), still lattice-matched to InP substrate, yielded k of 0.05-0.08 [11] and $F < 2$ for gains up to 25 [12]. Another example are AlInAsSb APDs exhibited effective k of 0.01-0.05 [13], [14] and 0.018 [15], depending on the exact composition.

In addition, AlGaAsSb diodes show low temperature coefficient of breakdown voltage, $C_{bd} = 0.86$ -0.91 mV/K [16] and high temperature and temporal stability [17]. A SAM-APD with InGaAs absorption region and AlAsSb avalanche region with a $C_{bd} \sim 8$ mV/K was reported [18]. This was lower than

Manuscript received February 27, 2022; revised April 01, 2022; accepted April 04, 2022. We are grateful for funding from the UK-Engineering and Physical Sciences Research Council grants (EP/N020715/1 and EP/K001469/1). The wafers were grown by the National Epitaxy Facility, at the University of Sheffield, UK. Ye Cao would like to thank Jonathan Taylor-Mew for the insightful discussion and Yuting Ji for helping in photoresponse spectrum measurement. (Corresponding author: Chee Hing Tan).

Ye Cao, Tarick Osman, Jo Shien Ng and Chee Hing Tan are with the Department of Electronic and Electric Engineering, The University of

Sheffield, Sheffield, S1 3JD, U.K. (email: ycao51@sheffield.ac.uk; tosmann2@sheffield.ac.uk; j.s.ng@sheffield.ac.uk; c.h.tan@sheffield.ac.uk).

Edmund Clarke and Pallavi Kisan Patil are with the EPSRC National Epitaxy Facility, The University of Sheffield, Sheffield, S3 7HQ, U.K. (edmund.clarke@sheffield.ac.uk; p.patil@sheffield.ac.uk).

The data reported in this article is available from the ORDA digital repository (<https://doi.org/10.15131/shef.data.19165943>).

typical values from various SAM-APDs with InP and InAlAs avalanche regions [19].

Although InGaAs/AlAsSb SAM-APD has been demonstrated [18], the large conduction band offset between InGaAs and AlAsSb (estimated to be 1.6 eV for Γ valleys [20]) necessitates a bandgap grading scheme using multiple layers of InAlGaAs and InAlAs within the APD. A promising alternative material for the absorption region is GaAs_{0.52}Sb_{0.48} (hereafter referred to as GaAsSb). It is lattice-matched to InP substrates and has a narrow bandgap for photon absorption up to 1.6 μm wavelength [21]. Crucially, the conduction band offset between GaAsSb and AlAsSb was estimated to be ~ 1.27 eV [22]. When combined with an AlGaAsSb avalanche region, a grading scheme with the Al composition gradually increasing can be used in the APD to bridge the conduction band offset from GaAsSb to AlGaAsSb.

In this paper, we assess experimentally the suitability of GaAsSb absorbers for SAM-APDs through demonstrating a GaAsSb/AlGaAsSb SAM-APD. APD characterization includes electrical characteristics and temperature dependent avalanche gain.

II. EXPERIMENTAL DETAILS

Structure of the APD wafer used in this work is shown schematically in Fig. 1. The wafer was grown on an n-type InP (100) substrate by molecular beam epitaxy. Be and Si were used as the p- and n-type dopants, respectively. The p⁺⁺ GaAsSb and n⁺⁺ InGaAs contact layers were nominally doped at $5 \times 10^{18} \text{ cm}^{-3}$. A bandgap grading scheme using Al_{1-x}Ga_xAs_{0.56}Sb_{0.44} (x decreasing from 0.8 to 0.2) was included between the narrow bandgap undoped (u.d) GaAsSb absorption region and the wide bandgap AlGaAsSb avalanche region.

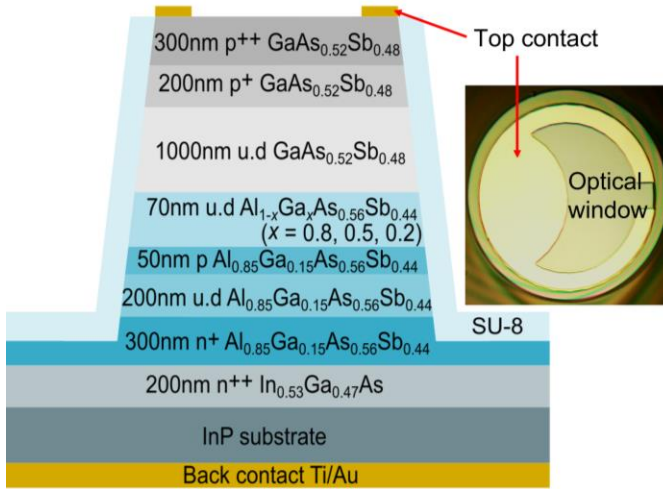


Fig. 1. Schematic cross section of GaAsSb/AlGaAsSb SAM-APD and top view of the fabricated 100 μm radius device.

Using standard photolithography techniques and wet chemical etching, the wafer was fabricated into circular mesa diodes with optical windows. The diodes had radius of 200, 100, 50 or 25 μm . A phosphoric based solution was used in the etching to create the mesa diodes by etching down to the n⁺ AlGaAsSb layer. The diodes had annular top contacts and back contacts formed by Ti/Au (20/200 nm). The mesa sidewall was covered by SU-8 negative photoresist.

A Keithley 236 source-measure-unit provided forward or reverse voltage biases to and measured the current-voltage (I-V) from the device-under-test (DUT). Capacitance-voltage (C-V) data were obtained, using an HP4275 LCR meter. The C-V data were analyzed using a 1-D Poisson solver to estimate the doping profile. In the analyses, we adjusted the doping concentration and thickness of each layer so that the C-V calculated by the Poisson solver matches the experimental C-V characteristics. Temperature dependent measurements were performed on the DUTs at temperatures of 295, 250, 200, 150 and 77 K using a low temperature probe station.

For avalanche gain measurements, the DUTs were illuminated by laser light at 1.55 μm wavelength. Phase-sensitive detection technique was used to ensure that the measurements were unaffected by the DUTs' dark current. This required modulated laser light and a lock-in amplifier to detect the resultant photocurrent. Care was also taken to focus the laser light within the DUTs' optical window. The laser power was measured using a commercial InGaAs photodiode with a known responsivity.

A combination of a tungsten halogen lamp and monochromator was used to measure the photoresponse versus wavelength characteristics. Again, the optical signal was modulated, and a lock-in amplifier was included in the setup to facilitate phase-sensitive detection. The photoresponse data were calibrated using the optical system response. Due to the larger optical spot size on DUTs in this setup, photoresponse measurements were performed on larger devices (those with radius of 200 μm).

III. RESULTS

Example I-V characteristics obtained under dark and laser illumination conditions are shown in Fig. 2(a) as current density (current normalized to device area). The forward dark current density data (0 to +2 V) suggest that the Ti/Au metal contacts deposited on p⁺⁺ GaAsSb are sufficiently ohmic. The reverse dark current density and photocurrent density (under the 1.55 μm wavelength laser illumination of a 156 nW) show a step increase at -6.5 V, followed by a gradual increase until -48 V. In general, there are some small disagreements in the reverse dark current density at biases below -45 V, indicating the presence of surface leakage currents. The dark current density data from different-sized devices at bias above -45 V show much better agreement, indicating the dominance of a bulk dark current mechanism.

To further investigate the dark current characteristics, dark current measurements were taken with DUTs' operating temperatures between 295 to 77 K. Temperature dependent data for a 100 μm radius device are shown in Fig. 2(b). At biases below -30 V, the dark current drops rapidly with temperature. However, at biases above -40 V, the dark current rises exponentially with the bias voltage, and shows weak temperature dependence, suggesting the presence of band-to-band tunnelling current. A sharp rise in the dark current was observed at 77 K at biases above -47 V, which is attributed to the onset of avalanche gain.

The step in the photocurrent near -6.5 V observed in Fig. 2(a) is attributed to an increase in the collection efficiency of photogenerated carriers when the depletion region extends into the GaAsSb absorption region, commonly referred to as punch-through. This is supported by C-V characteristics, which is shown in Fig. 3. A sudden decrease in capacitance, indicating a large increase in the depletion width, is observed at -5 V. Beyond -6 V, the capacitance remains almost constant, indicating a minimal change in the depletion width. These observations are consistent with the punch-through voltage \sim 6.5 V observed from gain measurements.

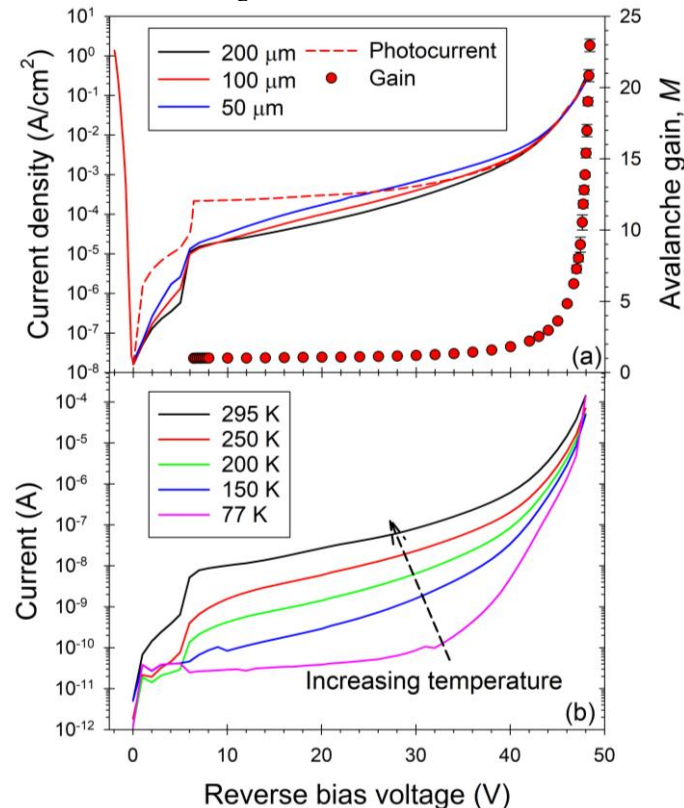


Fig. 2. (a) Dark current density of 200, 100 and 50 μm radius devices (solid lines), photocurrent density of 100 μm radius device (red dash line) and mean gain with standard deviation of three 100 μm radius devices at room temperature (b) temperature dependent dark current characteristics of 100 μm radius devices.

The experimental C-V characteristics were analyzed using a 1D Poisson's electric field solver. The dielectric constants for AlGaAsSb and GaAsSb were assumed to be 11.41 and 14.04 respectively, given by linear interpolation of values for GaAs, GaSb, AlAs and AlSb [23]. C-V fitting and the combination of doping density and thickness used are shown in Fig. 3.

The associated electric field profiles at selected biases are shown in Fig. 4. Our predicted electric field profiles suggest that the electric field in the GaAsSb absorption layer exceeds 200 kV/cm at biases above -32 V. At -40 and -48 V, the field increases to 275 and 340 kV/cm. These are relatively high electric field values for GaAsSb, whose bandgap is close to that of InGaAs. Hence the C-V analysis supports our deduction from Fig. 2 that band to band tunnelling current dominates at biases above -40 V. In future APD wafers, the electric field in the GaAsSb absorption layer can be reduced by increasing the

doping density or the thickness of the AlGaAsSb field control layer.

We now turned our focus to data of responsivity and avalanche gain. Fig. 5 shows the responsivity versus wavelength characteristics with the DUT reverse-biased at punch-through voltage. A mean responsivity of 0.39 A/W at 1.55 μm wavelength was obtained from four DUTs. Assuming 32% of air/semiconductor surface reflection loss and 1365 nm total absorption thickness, the absorption coefficient of the GaAsSb region was deduced as \sim $4.5 \times 10^3 \text{ cm}^{-1}$ at 1.55 μm wavelength. Peak responsivity of 0.40 A/W was observed at 1.50 μm wavelength. The cut-off wavelength, defined at 10% of the peak responsivity, is \sim 1.70 μm . This confirms that GaAsSb is a suitable absorption material to cover near-infrared wavelengths. The responsivity value can be increased by depositing an antireflection coating and/or increasing the thickness of the GaAsSb absorption region.

Room temperature avalanche gain values were extracted from phase-sensitive detected photocurrent data, using photocurrent value at -6.5 V as the unity gain reference value. The data are shown in Fig. 2(a), with a maximum mean gain value of \sim 23 at -48.4 V.

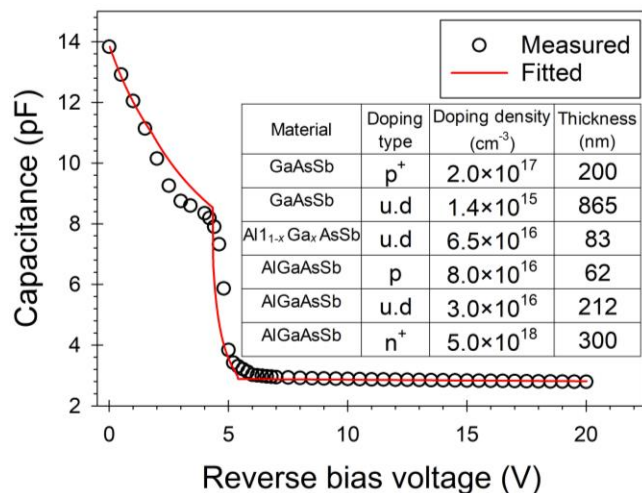


Fig. 3 Measured mean capacitance of three 100 μm radius devices and fitting versus reverse bias voltage. The fitting used assumed a built-in voltage of -1.2 V and parameter values in the inset table.

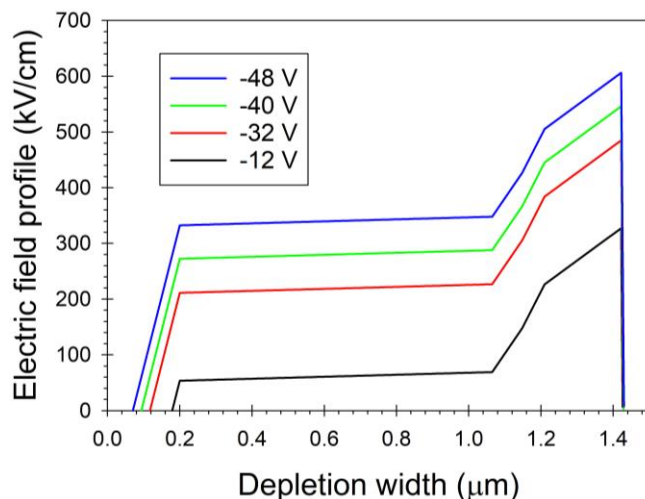


Fig. 4 Electric field profiles at -12, -32, -40 and -48 V, based on the C-V fitting.

Temperature dependence data of avalanche gain are shown in Fig. 6. As temperature decreases the dark current decreases, allowing the APDs to achieve higher gain. For a given reverse bias, the avalanche gain increases as temperature decreases, breakdown voltage was extracted from avalanche gain data, by linearly extrapolating $1/M$ to the reverse bias axis. The breakdown voltage decreases from 48.95 V at 295 K to 48.06 V at 77 K, producing $C_{bd} = (4.31 \pm 0.33)$ mV/K, as shown in the inset of Fig. 6.

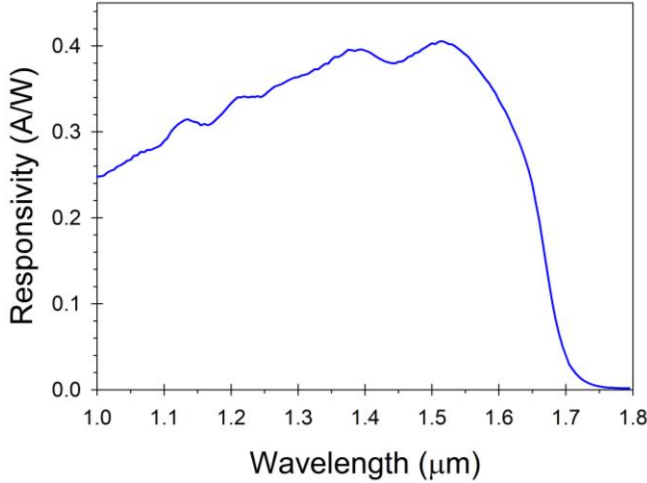


Fig. 5 Responsivity versus wavelength of 200 μm radius device biased at punch-through voltage under room temperature condition.

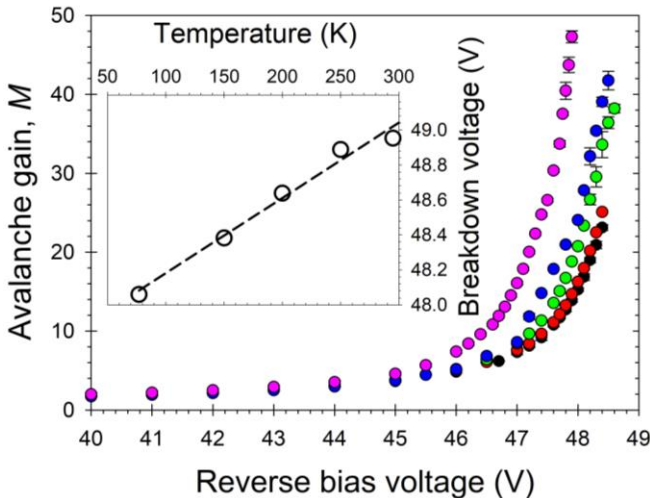


Fig. 6 Temperature dependent of mean avalanche gain with a standard deviation of three 100 μm radius devices under 295 K (black), 250 K (red), 200 K (green), 150 K (blue) and 77 K (pink). Inset shows the linear fitting for the temperature coefficient of breakdown voltage, $C_{bd} = (4.31 \pm 0.33)$ mV/K.

To the best of our knowledge, the C_{bd} value of this work is the lowest among SAM-APDs grown on InP substrates, as summarised in Fig. 7. The C_{bd} can be further reduced by reducing the avalanche region width, however, the width cannot be reduced indefinitely. In InP and InAlAs APDs, the onset of the band-to-band tunnelling current from narrow avalanche regions place a lower limit on the avalanche region width. Compared to SAM-APDs with similar avalanche region widths (200 nm), our GaAsSb/AlGaAsSb SAM-APD produces a C_{bd} value that is ~ 10 times and 5 times lower than that of InGaAs/InP and InGaAs/InAlAs SAM-APDs respectively. Our

C_{bd} value is also lower than that for the AlInAsSb grown on GaSb [28]. Therefore, GaAsSb absorption region can be combined with the AlGaAsSb avalanche region to produce SAM-APD with low temperature coefficient of breakdown voltage.

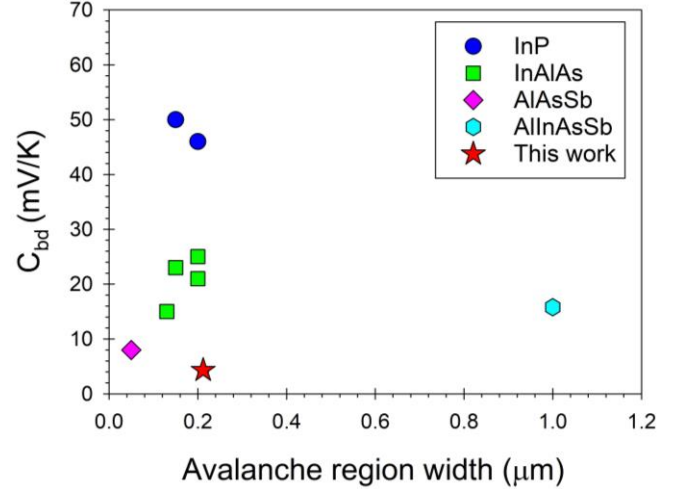


Fig. 7 Comparison temperature coefficient of breakdown voltage of this work with reported data for other SAM-APDs utilizing InP [19], [24], InAlAs [19], [25]-[27], AlAsSb [18], and AlInAsSb [28] avalanche region.

IV. CONCLUSION

We demonstrated a new SAM-APD structure consisting of a GaAsSb absorption and an AlGaAsSb avalanche region. The reverse dark current characteristics show presence of surface leakage current at low bias and tunnelling current at higher biases. The former suggests improved surface etching and passivation is needed whereas the latter indicates that the doping profile needs to be improved to reduce the tunnelling current.

The APD exhibited a responsivity of 0.39 A/W at 1.55 μm , a peak responsivity of 0.40 A/W at 1.50 μm and a cut-off wavelength of 1.70 μm . This shows that GaAsSb and AlGaAsSb can be an effective combination for infrared SAM-APD.

Temperature dependent avalanche gain data yield a very small temperature coefficient of breakdown voltage at 4.31 ± 0.33 mV/K, which is the smallest among reported SAM-APDs grown on InP substrates. Avalanche gain > 20 was obtained in all devices at each temperature.

REFERENCES

- [1] R. J. McIntyre, "Multiplication Noise in Uniform Avalanche Diodes," *IEEE Trans. Electron Devices*, vol. ED-13, no. 1, 1966, doi: 10.1109/T-ED.1966.15651..
- [2] T. Kaneda, "Silicon and Germanium Avalanche Photodiodes," *Semicond. Semimetals*, vol. 22, no. PD, pp. 247–328, Jan. 1985, doi: 10.1016/S0080-8784(08)62954-3.
- [3] A. R. J. Marshall, J. P. R. David, and C. H. Tan, "Impact ionization in InAs electron avalanche photodiodes," *IEEE Trans. Electron Devices*, vol. 57, no. 10, 2010, doi: 10.1109/TED.2010.2058330.
- [4] J. Beck *et al.*, "The HgCdTe electron avalanche photodiode," *LEOS Summer Top. Meet.*, vol. 5564, pp. 36–37, 2006, doi: 10.1117/12.565142.
- [5] N. Susa, H. Nakagome, O. Mikami, H. Ando, and H. Kanbe, "New InGaAs/InP Avalanche Photodiode Structure for the 1-1.6 μm Wavelength Region," *IEEE J. Quantum Electron.*, vol. 16, no. 8, pp. 864–

- 870, 1980, doi: 10.1109/JQE.1980.1070588.
- [6] S. Xie, S. Zhang, and C. H. Tan, "InGaAs/InAlAs Avalanche Photodiode with Low Dark Current for High-Speed Operation," *IEEE Photonics Technol. Lett.*, vol. 27, no. 16, pp. 1745–1748, 2015, doi: 10.1109/LPT.2015.2439153.
- [7] L. W. Cook, G. E. Bulman, and G. E. Stillman, "Electron and hole impact ionization coefficients in InP determined by photomultiplication measurements," *Appl. Phys. Lett.*, vol. 40, no. 7, 1982, doi: 10.1063/1.93190.
- [8] Y. L. Goh *et al.*, "Avalanche multiplication in InAlAs," *IEEE Trans. Electron Devices*, 2007, doi: 10.1109/TED.2006.887229.
- [9] X. Yi *et al.*, "Extremely low excess noise and high sensitivity AlAs_{0.56}Sb_{0.44} avalanche photodiodes," *Nat. Photonics*, vol. 13, no. 10, pp. 683–686, 2019, doi: 10.1038/s41566-019-0477-4.
- [10] J. Xie, S. Xie, R. C. Tozer, and C. H. Tan, "Excess noise characteristics of thin AlAsSb APDs," *IEEE Trans. Electron Devices*, 2012, doi: 10.1109/TED.2012.2187211.
- [11] L. L. G. Pinel *et al.*, "Effects of carrier injection profile on low noise thin Al_{0.85}Ga_{0.15}As_{0.56}Sb_{0.44} avalanche photodiodes," *Opt. Express*, vol. 26, no. 3, p. 3568, 2018, doi: 10.1364/oe.26.003568.
- [12] J. Taylor-Mew, V. Shulyak, B. White, C. H. Tan, and J. S. Ng, "Low Excess Noise of Al_{0.85}Ga_{0.15}As_{0.56}Sb_{0.44} Avalanche Photodiode from Pure Electron Injection," *IEEE Photonics Technol. Lett.*, vol. 1135, no. c, pp. 1–1, 2021, doi: 10.1109/lpt.2021.3110123.
- [13] M. Ren, S. J. Maddox, M. E. Woodson, Y. Chen, S. R. Bank, and J. C. Campbell, "AllInAsSb separate absorption, charge, and multiplication avalanche photodiodes," *Appl. Phys. Lett.*, vol. 108, no. 19, pp. 10–14, 2016, doi: 10.1063/1.4949335.
- [14] M. Ren, S. J. Maddox, M. E. Woodson, Y. Chen, S. R. Bank, and J. C. Campbell, "Characteristics of Al_{1-x}Ga_xAs_{0.56}Sb_{1-y} (x:0.3–0.7) Avalanche Photodiodes," *J. Light. Technol.*, vol. 35, no. 12, pp. 2380–2384, Jun. 2017, doi: 10.1109/JLT.2017.2681041.
- [15] S. H. Kodati *et al.*, "AllInAsSb avalanche photodiodes on InP substrates," *Appl. Phys. Lett.*, vol. 118, no. 9, 2021, doi: 10.1063/5.0039399.
- [16] X. Zhou *et al.*, "Thin Al_{1-x}Ga_xAs_{0.56}Sb_{0.44} diodes with extremely weak temperature dependence of avalanche breakdown," *R. Soc. Open Sci.*, vol. 4, no. 5, 2017, doi: 10.1098/rsos.170071.
- [17] S. Abdullah, C. H. Tan, X. Zhou, S. Zhang, L. Pinel, and J. S. Ng, "Investigation of temperature and temporal stability of AlGaAsSb avalanche photodiodes," *Opt. Express*, vol. 25, no. 26, p. 33610, 2017, doi: 10.1364/oe.25.033610.
- [18] J. Xie, J. S. Ng, and C. H. Tan, "An InGaAs/AlAsSb avalanche photodiode with a small temperature coefficient of breakdown," *IEEE Photonics J.*, vol. 5, no. 4, 2013, doi: 10.1109/JPHOT.2013.2272776.
- [19] L. J. J. Tan *et al.*, "Temperature Dependence of Avalanche Breakdown in InP and InAlAs," *IEEE J. Quantum Electron.*, vol. 46, no. 8, pp. 1153–1157, 2010.
- [20] K. A. Romanova and Y. G. Galyametdinov, "Theoretical simulation of quantum cascade lasers based on InGaAs/AlInAs and InGaAs/AlAsSb quantum wells," in *IOP Conference Series: Materials Science and Engineering*, 2020, vol. 862, no. 2, doi: 10.1088/1757-899X/862/2/022040.
- [21] M. S. Park and J. H. Jang, "GaAs_{0.5}Sb_{0.5} lattice matched to InP for 1.55 μm photo-detection," *Electron. Lett.*, vol. 44, no. 8, pp. 40–41, 2008, doi: 10.1049/el.
- [22] O. Ostinelli, G. Almuneau, and W. Bächtold, "Photoluminescence and band offset of type-II AlGaAsSb/InP heterostructures," *Semicond. Sci. Technol.*, vol. 21, no. 5, pp. 681–685, 2006, doi: 10.1088/0268-1242/21/5/020.
- [23] A. De and C. E. Pryor, "Optical dielectric functions of wurtzite III-V semiconductors," *Phys. Rev. B - Condens. Matter Mater. Phys.*, vol. 85, no. 12, 2012, doi: 10.1103/PhysRevB.85.125201.
- [24] K. S. Hyun and C. Y. Park, "Breakdown characteristics in InP/InGaAs avalanche photodiode with p-i-n multiplication layer structure," *J. Appl. Phys.*, vol. 81, no. 2, pp. 974–984, 1997, doi: 10.1063/1.364225.
- [25] B. F. Levine *et al.*, "A new planar InGaAs-InAlAs avalanche photodiode," *IEEE Photonics Technol. Lett.*, vol. 18, no. 18, 2006, doi: 10.1109/LPT.2006.881684.
- [26] A. Rouvié, D. Carpentier, N. Lagay, J. Décobert, F. Pommereau, and M. Achouche, "High gain × bandwidth product over 140-GHz planar junction AllnAs avalanche photodiodes," *IEEE Photonics Technol. Lett.*, vol. 20, no. 6, 2008, doi: 10.1109/LPT.2008.918229.
- [27] E. Ishimura *et al.*, "Degradation mode analysis on highly reliable guardring-free planar InAlAs avalanche photodiodes," *J. Light. Technol.*, vol. 25, no. 12, 2007, doi: 10.1109/JLT.2007.909357.
- [28] A. H. Jones, Y. Yuan, M. Ren, S. J. Maddox, S. R. Bank, and J. C. Campbell, "Al_xIn_{1-x}As_ySb_{1-y} photodiodes with low avalanche breakdown temperature dependence," *Opt. Express*, vol. 25, no. 20, p. 24340, 2017, doi: 10.1364/oe.25.024340.

Ye Cao received the B.Eng. degree from the Nanjing Normal University, Nanjing, China, in 2018 and the MSc. degree in electronic and electric engineering from The University of Sheffield, Sheffield, UK, in 2019 where he is pursuing a Ph.D. degree. His research interests include design and characterization of infrared avalanche photodiodes.

Tarick Osman received the B.Eng. degree in electronic and electrical engineering from the University of Sheffield, U.K., in 2019 where he is currently pursuing a Ph.D. degree. His current research interests include design, fabrication, and characterization of avalanche photodiodes for infrared applications.

Edmund Clarke received the B.Sc. degree in physics and the Ph.D. degree in physics from Imperial College London, London, U.K., in 1996 and 2005, respectively. He was a Research Associate at Imperial College London for five years, where he was involved in the research on molecular beam epitaxy of quantum dot devices. In October 2010, he joined the University of Sheffield, U.K., where he is currently a Senior Research Fellow and is responsible for III–V semiconductor growth by molecular beam epitaxy for the EPSRC National Epitaxy Facility.

Pallavi Kisan Patil received a Doctor of Engineering degree from Ehime University, Matsuyama, Japan in 2017 and subsequently was a postdoctoral researcher at the Kyoto Institute of Technology, Japan. In 2018 she joined the University of Sheffield, U.K., where she is currently a Research Associate based in the EPSRC National Epitaxy Facility, working on molecular beam epitaxy growth of III-V semiconductors.

Jo Shien Ng (M'99) received the B.Eng. and Ph.D. degrees in electronic engineering from the University of Sheffield, Sheffield, U.K., in 1999 and 2003, respectively.

She is currently a Professor of semiconductor devices with the Department of Electronic and Electrical Engineering, University of Sheffield. She was a Royal Society Research Fellow based in the same department between 2006 and 2016.

She has authored or co-authored nearly 90 peer-reviewed journal articles. Her research interests include avalanche photodiodes, Geiger mode avalanche photodiodes, and material characterization.

Chee Hing Tan (M'95 -SM'17) received the B.Eng. and Ph.D. degrees in electronic engineering from the Department of Electronic and Electrical Engineering, University of Sheffield, Sheffield, U.K., in 1998 and 2002, respectively.

He is currently a Professor of Opto-electronic Sensors and the Head of Department at the Department of Electronic and Electrical Engineering, University of Sheffield.

He has extensive experience in the characterization and modeling of high-speed low-noise avalanche photodiodes and phototransistors. His current research interests include novel semiconductor materials, single-photon avalanche diodes, infrared photodiodes, X-ray detectors, and ultrahigh-speed avalanche photodiodes.